for her aid in the preparation of this paper.

Registry No. PS (homopolymer), 9003-53-6; PVME (homopolymer), 9003-09-2.

References and Notes

(1) Paul, D. R.; Newman, S. *Polymer Blends*; Academic: New York, 1978; Vol. I and II.
(2) Olabisi, O.; Robeson, L. M.; Shaw, M. T. *Polymer–Polymer Miscibility*; Academic: New York, 1979.
(3) Martuscelli, E., Palumbo, R., Kryszewski, M., Eds. *Polymer Blends: Processing, Morphology and Properties*; Plenum: New York, 1980.
(4) Guinier, A. *X-ray Diffraction in Crystals, Imperfect Crystals and Amorphous Bodies*; Freeman: San Francisco, 1963.
(5) Alexander, L. E. *X-ray Diffraction Methods in Polymer Science*; Wiley: New York, 1969.
(6) Klug, H. P.; Alexander, L. E. *X-ray Diffraction Procedures of Polycrystalline and Amorphous Materials*; Wiley: New York, 1974.
(7) Spuriell, J. E.; Clark, E. S. *Methods Exp. Phys.* **1980**, *16*, 1.
(8) Wang, J.-I.; Harrison, I. R. *Methods Exp. Phys.* **1980**, *16*, 128.
(9) Blazek, A. *Thermal Analysis*; Van Nostrand Reinhold: Princeton, NJ, 1973.
(10) Vadimsky, R. G. *Methods Exp. Phys.* **1980**, *16*, 185.
(11) Nishi, T.; Wang, T. T. *Macromolecules* **1975**, *8*, 909.
(12) de Boer, A.; Challa, G. *Polymer* **1976**, *17*, 633.
(13) Boyer, R. F.; Spencer, R. S. *J. Appl. Phys.* **1944**, *15*, 398.
(14) Bohn, L. *Adv. Chem. Ser.* **1971**, *99*, 66.
(15) Marcincin, K.; Ramanov, A.; Pollak, V. *J. Appl. Polym. Sci.* **1972**, *16*, 2239.
(16) Wetton, R. E.; MacKnight, W. J.; Fried, J. R.; Karasz, F. E. *Macromolecules* **1978**, *11*, 158.
(17) Mehra, U.; Toy, L.; Biliyar, K.; Shen, M. *Adv. Chem. Ser.* **1975**, *142*, 399.
(18) McCall, D. W.; Douglass, D. C. *Polymer* **1963**, *4*, 433.
(19) Douglass, D. C.; Jones, G. P. J. *J. Chem. Phys.* **1966**, *45*, 956.
(20) McBrierty, V. J.; Douglass, D. C.; Kwei, T. K. *Macromolecules* **1978**, *11*, 1265.
(21) McBrierty, V. J. *Faraday Discuss. Chem. Soc.* **1979**, *68*, 78.
(22) Lind, A. C. *J. Chem. Phys.* **1977**, *66*, 3482.
(23) Crist, B.; Peterlin, A. *J. Polym. Sci., Part A-2* **1969**, *7*, 1165.
(24) Douglass, D. C.; McBrierty, V. J. *J. Chem. Phys.* **1971**, *54*, 4085.
(25) Wardell, G. E.; McBrierty, V. J.; Douglass, D. C. *J. Appl. Phys.* **1974**, *45*, 3441.
(26) Caravatti, P.; Neuenschwander, P.; Ernst, R. R. *Macromolecules* **1985**, *18*, 119.
(27) Bank, M.; Leffingwell, J.; Thies, C. *Macromolecules* **1971**, *4*, 43.
(28) Bank, M.; Leffingwell, J.; Thies, C. *J. Polym. Sci.*, Part *A-2* **1972**, *10*, 1097.
(29) Kwei, T. K.; Nishi, T.; Roberts, R. F. *Macromolecules* **1974**, *7*, 667.
(30) Abragm, A. *The Principles of Nuclear Magnetism*, Clarendon Press: Oxford, 1961.
(31) Goldman, M.; Shen, L. *Phys. Rev.* **1966**, *144*, 321.
(32) Cheung, T. T. P.; Gerstein, B. C.; Ryan, L. M.; Taylor, R. E. *J. Chem. Phys.* **1980**, *73*, 6059.
(33) Havens, J. R.; VanderHart, D. L. 25th Experimental NMR Conference, Wilmington, DE, April 1984.
(34) Taylor, R. E.; Pembleton, R. G.; Ryan, L. M.; Gerstein, B. C. *J. Chem. Phys.* **1979**, *71*, 4541.
(35) Ryan, L. M.; Taylor, R. E.; Paff, A. J.; Gerstein, B. C. *J. Chem. Phys.* **1980**, *72*, 508.
(36) Scheler, G.; Haubenreisser, U.; Rosenberger, H. *J. Magn. Reson.* **1981**, *44*, 134.
(37) Caravatti, P.; Levitt, M. H.; Ernst, R. R. *J. Magn. Reson.*, in press.
(38) Forsén, S. H.; Hoffman, R. A. *J. Chem. Phys.* **1963**, *39*, 2892.
(39) Forsén, S. H.; Hoffman, R. A. *J. Chem. Phys.* **1966**, *45*, 2049.
(40) Noggle, J. H.; Schirmer, R. E. *The Nuclear Overhauser Effect, Chemical Applications*; Academic Press: New York, 1971.
(41) Kalk, A.; Berendsen, H. J. C. *J. Magn. Reson.* **1976**, *24*, 343.
(42) Gordon, S. L.; Wüthrich, K. *J. Am. Chem. Soc.* **1978**, *100*, 7094.
(43) Wagner, G.; Wüthrich, K. *J. Magn. Reson.* **1979**, *33*, 675.
(44) Bothner-By, A. A. In *Magnetic Resonance Studies in Biology*; Shulman, R. G., Ed.; Academic: New York, 1979.
(45) Caravatti, P.; Bodenhausen, G. Ernst, R. R. *J. Magn. Reson.* **1983**, *55*, 88.
(46) Rhim, W. K.; Elleman, D. D.; Vaughan, R. W. *J. Chem. Phys.* **1973**, *58*, 1772.
(47) Mansfield, P. *J. Phys. C.* **1971**, *C4*, 1444.

^{13}C NMR Study of the Sequence Distribution of Poly(acrylamide-*co*-sodium acrylates) Prepared in Inverse Microemulsions

Françoise Candau* and Zoubir Zekhnini

Institut Charles Sadron (CRM-EAHP), CNRS-ULP Strasbourg, 67083 Strasbourg Cedex, France

Frank Heatley

Department of Chemistry, University of Manchester, Manchester, M13 9PL, U.K.
Received December 2, 1985

ABSTRACT: The microstructure of poly(acrylamide-*co*-sodium acrylates) of variable compositions and prepared by inverse microemulsion polymerization was studied by ^{13}C NMR. The average copolymer composition is shown to be independent of the degree of conversion, and the sequence monomer distribution analyzed from triad proportions conforms to Bernouillian statistics within experimental error. The reactivity ratios of both monomers are therefore close to unity, a significant difference from the reported literature values obtained for copolymers prepared in solution or inverse emulsion ($r_A \sim 0.3$; $r_M \sim 0.95$). These results confirm a polymerization process by nucleation and interparticular collisions rather than by monomer diffusion through the continuous medium.

Introduction

Over the past 20 years, there have been numerous studies of the influence of the reaction medium on the free-radical copolymerization of acrylamide with ionogenic monomers, e.g., acrylic and methacrylic acids. Two detailed reviews have been published recently.[1,2] Among the factors controlling monomer reactivity are hydrogen bonding, dipolar interactions and electrostatic forces, and EDA complex formation. Consequently, the kinetics of the reaction as well as the microstructure of the resulting

0024-9297/86/2219-1895$01.50/0

polymers greatly depend on the pH of the medium, the nature of the solvent, the monomer concentration, and the presence of surfactants and complexing agents.

The reactivity ratios of acrylamide and acrylic acid have been determined for copolymers obtained in homogeneous aqueous solution[3-7] and emulsion[9] as a function of pH. For solution polymerization, on increasing the pH from 2 to 9, the reactivity ratio of acrylic acid (r_A) decreases from 1.7 to 0.3, whereas that of acrylamide (r_M) increases from 0.3 to 0.95.

In the case of emulsion polymerization[9] the reactivity of the monomers depends in addition upon their partition coefficient between the organic and aqueous phases. More specifically, at low pH an important part of the acrylic or methacrylic acid is in the organic phase, the proportion being a function of the comonomer composition. As a result, the reactivity parameters ($r_M = 0.58$, $r_A = 3.80$) are quite different from those obtained in solution ($r_M = 0.20$; $r_A = 2.8$).[7] On the other hand, at high pH (pH 10) almost all of the monomers are confined within the particles, and no correction for partition is necessary. The reactivity parameters ($r_M = 1.06$; $r_A = 0.29$) are therefore very close to those obtained in homogeneous solution ($r_M = 0.95$; $r_A = 0.3$).[7]

Recently, Candau et al.[10,11] have described a new method of synthesis of acrylamide and derivatives using a microemulsion polumerization procedure. Microemulsions are essentially transparent and thermodynamically stable oil/water systems stabilized by one or two surface active agents.[12] Polymerization in inverse microemulsion was shown to lead to remarkably stable clear latexes of low particle size ($d < 60$ nm) containing up to 25% of copolymers in the medium, in contrast to inverse latexes prepared by using classical emulsions that are often unstable and turbid.[13-15]

The purpose of the present work was to determine the reactivity parameters of the copolymers prepared by microemulsion polymerization for comparison with those from solution and emulsion polymerization. The microstructure of the poly(acrylamide-*co*-acrylates) was determined by ^{13}C NMR, which enabled us to analyze the monomer sequence distribution up to triads and to compare it with statistical models.

Experimental Section

^{13}C NMR. ^{13}C spectra were run between 19 and 80 °C by using a Varian Associates Fourier transform XL-300 spectrometer operating at 75.5 MHz with broadband proton decoupling. Solutions in D_2O contained ca. 40 mg cm^{-3} of polymer. The RF pulse interval was normally set at 0.4 s, with a flip angle of 24° and a spectral width of 15 000 Hz. Resolution enhancement was carried out by using the Lorentz–Gaussian transformation technique.[16]

Samples. The transparent and thermodynamically stable microemulsions were prepared with stirring by adding the aqueous solution of monomers (neutralized at pH 9–10) to the mixture of nonionic emulsifiers (a sesquioleate sorbitan + a poly(oxyethylene)sorbitol hexaoleate). More details are given in ref 11.

One series of copolymers was prepared under UV irradiation at 20 °C in the absence of any photosensitizer. All other series were synthesized thermally at 45 °C with AIBN as the initiator.

In the case of polymerizations to be stopped at low conversion levels, the reaction was followed dilatometrically[17] and stopped at the appropriate point by precipitation of the latex in a 50–50 acetone–methanol mixture maintained at 5 °C and containing hydroquinone inhibitor. The copolymer was washed several times with methanol, filtered, and dried under vacuum at 45 °C.

Theoretical Section

For convenience, we summarize here the essentials of the statistics of copolymer sequence structure[18,19] as required for the present problem. Let A and M denote acrylate and acrylamide units, respectively. The relative proportions of monomer, diad, and triad sequences are related by

$$(A) = (AA) + \tfrac{1}{2}(AM) = (AAA) + (AAM) + (MAM)$$

$$(M) = (MM) + \tfrac{1}{2}(AM) = (MMM) + (MMA) + (AMA)$$

$$(AA) = (AAA) + \tfrac{1}{2}(AAM)$$

$$(AM) = (AAM) + 2(MAM) = (MMA) + 2(AMA)$$

$$(MMA) + 2(AMA)$$

$$(MM) = (MMM) + \tfrac{1}{2}(MMA)$$

(Note that the relative intensity of an unsymmetrical sequence, e.g., (AAM), also includes the inverse (MAA)).

In the Bernouillian model there is one independent probability, that of adding, say, an A unit, P_A. Necessarily $P_A + P_M = 1$. The monomer and triad intensities are related to P_A by

$$(AAA) = P_A^3 \qquad (AMA) = P_A^2(1 - P_A)$$

$$(AAM) = 2P_A^2(1 - P_A) \qquad (MMA) = 2P_A(1 - P_A)^2$$

$$(MAM) = P_A(1 - P_A)^2 \qquad (MMM) = (1 - P_A)^3$$

This model implies the existence of only two propagation steps

$$(\sim)^\bullet_n + A \xrightarrow{k_A} (\sim)^\bullet_{n+1}$$

$$(\sim)^\bullet_n + M \xrightarrow{k_M} (\sim)^\bullet_{n+1}$$

giving

$$P_A = rf_A/[1 + f_A(r - 1)]$$

where $r = k_A/k_M$ and f_A is the mole fraction of A in the comonomer feed.

In the first-order Markov model, the addition probability depends on the end unit of the growing chain. There are four conditional probabilities, P_{XY}, where X denotes the end unit and Y the added unit (X, Y = A or M). Only two probabilities are independent since necessarily $P_{AA} + P_{AM} = P_{MM} + P_{MA} = 1$. Defining $u = P_{AM}$ and $w = P_{MA}$, one obtains

$$(AAA) = w(1 - u)^2/(u + w) \qquad (AMA) = uw^2/(u + w)$$

$$(AAM) = 2uw(1 - u)/(u + w)$$

$$(MMA) = 2uw(1 - w)/(u + w)$$

$$(MAM) = u^2w/(u + w)$$

$$(MMM) = u(1 - w)^2/(u + w)$$

This model corresponds to four distinct propagation steps of general form

$$\sim X\cdot + Y \xrightarrow{k_{XY}} \sim Y\cdot$$

giving

$$u = (1 - f_A)/[1 + f_A(r_A - 1)]$$

$$w = f_A/[r_M + f_A(1 - r_M)]$$

where r_A and r_M (the reactivity ratios) are equal to k_{AA}/k_{AM} and k_{MM}/k_{MA}, respectively. If $r_A = r_M = 1$ (and hence $P_{AM} + P_{MA} = 1$), first-order Markov statistics reduce to the Bernouillian case.

Results

Previous NMR studies[20-22] of acrylamide (M) and acrylate (A) homopolymers have shown that the C=O

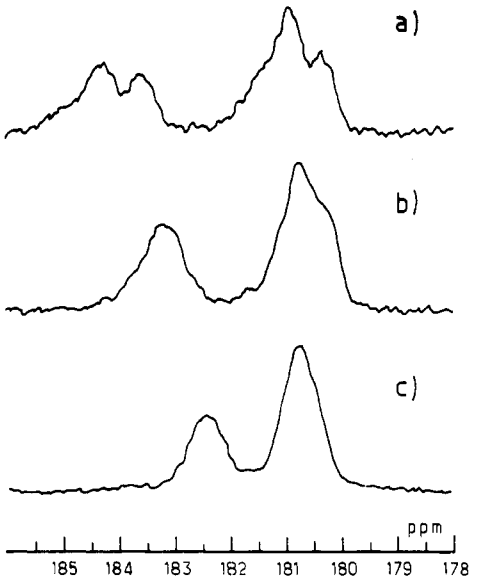

Figure 1. ^{13}C NMR spectrum of the carbonyl carbon of copolymer AB-1: (a) copolymer as isolated, 80 mg of polymer in 2 cm^3 D_2O; (b) 0.1 cm^3 N NaOH added to original; (c) 0.2 cm^3 added to original. No resolution enhancement has been applied.

peak is essentially unaffected by tacticity, whereas the CH and CH_2 resonances are split into several peaks. In copolymers[3] the CH and C=O peaks are clearly split into A and M regions, whereas the CH_2 region is relatively unchanged. In all our samples, the (A) and (M) CH peaks were centered at δ 46.0 and 43.0, respectively, and the (M) C=O peak occurred at δ 181 ± 0.5. However, the position of the (A) C=O resonance varied irregularly from sample to sample within the range δ 180–185. These fluctuations were found to be associated with varying degrees of neutralization of the acrylate units; this effect was also revealed by elemental analysis.[23] Because of rapid proton exchange, the C=O chemical shift of A groups is averaged

$$\bar{\delta}_A = \delta_{CO_2H}P_{CO_2H} + \delta_{CO_2^-}P_{CO_2^-}$$

where P_X and δ_X are the probability and chemical shift of group X, respectively. From the spectra of acrylate and acrylic acid homopolymers, we calculate $\delta_{CO_2H} \sim 178.4$ and $\delta_{CO_2^-} \sim 185.1$. Figure 1 shows the typical evolution of a spectrum on addition of NaOH; it refers to sample AB-1, which originally was about 60% neutralized. For low neutralization degree the resolution is poor and only the monomer fractions can be obtained. For complete neutralization the A and M regions are fully resolved, and further splittings appear arising from triad sequences as described below. For each sample, an appropriate amount of NaOH was carefully added to give complete neutralization; an excess of alkali would partially hydrolyze the acrylamide units.[24] Such hydrolysis is apparent from a change in the monomer fractions. The triad intensities were only used if addition of alkali produced no hydrolysis.

The triad resolution was significantly improved by resolution enhancement (cf. Figures 1 and 2), allowing reasonably accurate analysis of the monomer sequence distribution up to the triad level. Resolution enhancement produced no change in the monomer fractions.

The standard conditions described in the Experimental Section were chosen to maximize the efficiency of signal accumulation for the C=O signal. However, the pulse interval chosen is shorter than the spin–lattice relaxation time of the carbonyl carbons, raising the possibility of inaccurate relative intensities because of differential relaxation of acrylamide and acrylate units. This possibility was checked in three ways for sample A-9 containing ca.

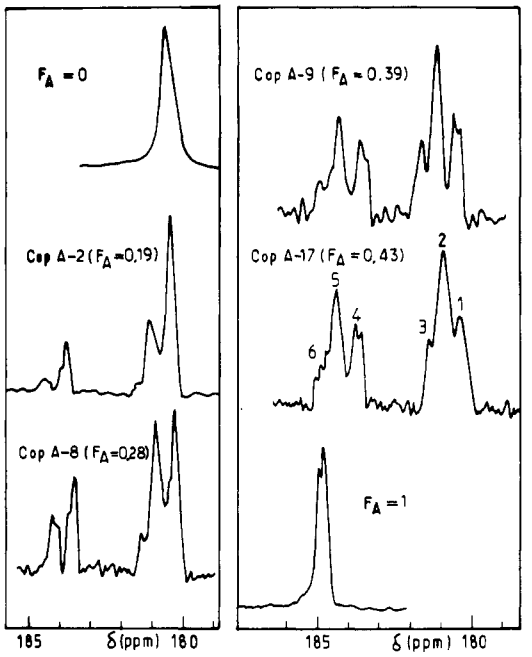

Figure 2. ^{13}C NMR spectra of the carbonyl carbon of acrylamide/acrylate polymers. The spectrum for $F_A = 0$ is polyacrylamide, and the spectrum for $F_A = 1$ is poly(sodium acrylate). Resolution enhancement has been applied to the copolymer spectra. The numbers on the spectrum of copolymer A-17 identify monomer triads: (1) MMM (δ 180.4); (2) MMA (181.0); (3) AMA (181.5); (4) MAM (183.9); (5) AAM (184.5); (6) AAA (185.1).

Table I
Monomer Compositions for Sample A-9 under Different Experimental Conditions

T, °C	pulse interval, s	flip angle	NOE	P_A C=O	P_A CH
20	0.4	24°	yes	0.394	0.392
80	0.4	24°	yes	0.385	0.389
20	4.4	73°	no	0.368	0.390

39 mol % acrylate. First, the monomer composition from the carbonyl region was compared with that from the CH region. Because of the attached protons, the relaxation times of ^{13}CH nuclei are much shorter than those of ^{13}C=O nuclei, and hence will give a different composition if differential relaxation is important. Second, a spectrum was run with a pulse interval of 4.4 s and a flip angle of 73° with the proton decoupler on only during the acquisition period of 0.4 s, thus suppressing the nuclear Overhauser enhancement. Third, a spectrum was run at 80 °C, where the relaxation times are longer than at 20 °C. The resulting compositions are given in Table I. There is no significant variation in the acrylate mole fraction F_A, and the peak intensities from standard spectra are therefore reliable.

We first examined the microstructure of two series of copolymers initiated photochemically (UV) or thermally (T = 45 °C) and characterized by high degrees of conversion ($Y > 90\%$). The results obtained led us to subsequently study series of copolymers of various compositions at different levels of conversion ($4\% < Y < 100\%$).

a. Poly(acrylamide-*co*-acrylates) Obtained at High Levels of Conversion. The characteristics of the samples are given in Table II. The mole fraction of sodium acrylate in the feed (f_A) and that in the final copolymer (F_A) are reported together with the percentage conversions (Y). The results show an excellent agreement between the values of f_A and F_A. Such agreement is expected logically for $Y = 100\%$. For $70\% < Y < 100\%$ significant devia-

Table II
Feed Compositions (f_A) and Copolymer Compositions (F_A) for High-Conversion Polymerizations (Y)

system[a]	Y, %	f_A	F_A	T,[c] °C
A-11(T)	90	0.097	0.130[b]	20
A-2(T)	93	0.198	0.186[b]	20
A-8(T)	94	0.296	0.298	20
			0.284[b]	20
A-14(T)	90	0.345	0.345	19
A-9(T)	89	0.397	0.385[b]	19
			0.394	19
			0.382[b]	80
			0.385	80
A-17(T)	74	0.445	0.426	20
			0.437[b]	20
A-19(T)	100	0.546	0.523[b]	20
A-30(P)	63.8	0.095	0.101	19
A-31(P)	63	0.177	0.177	19
			0.187	19
A-29(P)	100	0.247	0.230[b]	19
			0.259	19
A-25(P)	100	0.295	0.269	19
A-10(P)	90	0.356	0.342[b]	19
A-33(P)	77.7	0.569	0.533	19
			0.530	50

[a] (T) indicates thermal and (P) photochemical initiation. [b] Resolution-enhanced spectrum. [c] Temperature of NMR spectrum.

tions of F_A from f_A would occur only for reactivity ratios very different from 1. For a more detailed insight into the copolymerization kinetics, we now examine the sequence distribution as revealed by the triad proportions.

Figure 2 shows the development of the carbonyl resonance with increasing acrylate content for the thermally initiated series. The spectra of the homopolymers are also shown for comparison, and the triad assignment is indicated on the spectrum of A-17. This assignment has been deduced directly from the dependence of the component resonances on copolymer composition and a comparison with the homopolymer chemical shifts. It is in agreement with that reported previously for radical poly(acrylamide-*co*-acrylates) prepared in aqueous solution.[20]

Figures 3 and 4 show the comparison for both series between the experimental triad proportions and the theoretical distribution curves for Bernouillian statistics calculated by using the relationship $P_A = F_A$. In view of the fact that literature values of the reactivity ratios differ from unity (see Introduction), there is surprisingly good agreement between experiment and theory for this model. However, a recent analysis of Truong et al.[3] has shown that for high degrees of conversion an apparent distribution close to that of Bernouilli could be obtained when taking into account the compositional heterogeneity of poly(acrylamide-*co*-acrylates) with reactivity ratios $r_A = 0.3$ and $r_M = 0.95$.

A proper determination of the reactivity ratios of monomers requires therefore a sequence distribution analysis of copolymers with various compositions and degrees of conversion, particularly in the low conversion range (<-10%), where the average copolymer composition and the instantaneous composition correspond closely.

b. Poly(acrylamide-*co*-acrylates) Obtained over a Wide Conversion Range. Three series of given composition (series AK, $f_A \sim 0.23$; Z, $f_A \sim 0.29$; and AB, $f_A \sim 0.39$) were prepared by thermal initiation at 45 °C. Within each series, the degree of conversion varied from 4 to 100%. It should be noted that owing to the very fast rate of reaction successive samples could not be taken during the same experiment. Thus, each copolymer corresponds to a separate experiment. Two further samples, ZZ-II and

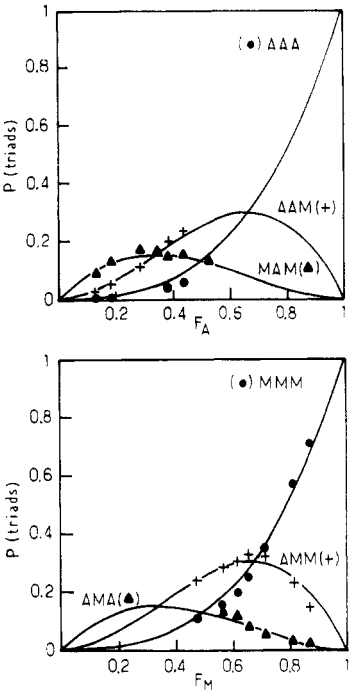

Figure 3. Comparison of experimental triad proportions (symbols) with those calculated for Bernouillian statistics with $P_A = F_A$ (curves), for samples of high conversion and thermal initiation (Table II).

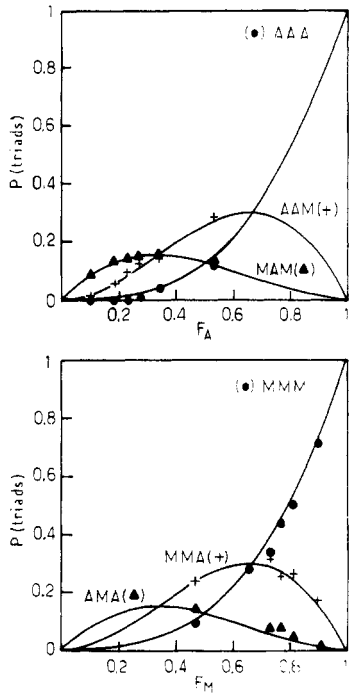

Figure 4. Legend as Figure 3 except photochemical initiation (Table II).

QY-I, were prepared to extend the composition range from $f_A = 0.15$ to $f_A = 0.53$.

The percentage conversions, comonomer feed compositions, and NMR copolymer compositions are given in Tables III and IV. There is good agreement between the acrylate content in the feed and in the copolymer obtained, whatever the degree of conversion, indicating the absence of a drift in the comonomer composition.

This is illustrated in Figure 5, which shows the variation of the average copolymer composition with conversion for each series. Horizontal lines are obtained within experimental error. For comparison, we also report the variation

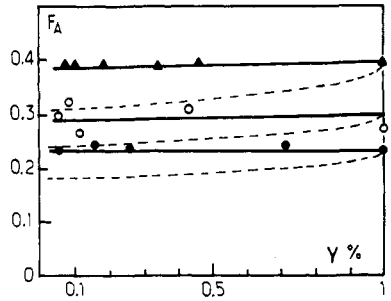

Figure 5. Variation of average copolymer composition F_A with degree of conversion Y for three values of f_A: (●) series AK, $f_A \sim 0.23$; (○) series CZ, $f_A \sim 0.29$; (▲) series AB, $f_A \sim 0.39$. The solid lines have been drawn through the experimental points. The dashed lines represent the calculated composition for emulsion copolymerization with $r_A = 0.29$ and $r_M = 1.06$ (ref 9).

Table III
Feed Compositions (f_A) and Copolymer Compositions (F_A) for Series Obtained over a Wide Conversion Range

system	Y, %	f_A	F_A	T,[c] °C
AB-3	8.5	0.391	0.399	19
			0.393[b]	19
AB-1	10.4	0.384	0.398	50
			0.420[b]	50
AB-4	18.8	0.390	0.394	18
			0.386[b]	18
AB-6	34.4	0.392	0.411	18
			0.396[b]	18
AB-2	46.6	0.391	0.380	50
			0.363[b]	50
AB-5	100	0.388	0.419[b]	50
1C-3Z	6.1	0.293	0.299	19
1C-4Z	8.5	0.296	0.325	19
C-1	11.4	0.292	0.262	19
1C-2Z	43.8	0.290	0.315	19
1C-5Z	100	0.290	0.272	19
ZZ-II	7.4	0.156	0.150	19
QY-I	9.6	0.531	0.514	19

[a] All samples thermally initiated. [b] Resolution-enhanced spectrum. [c] Temperature of NMR spectrum.

of the average composition calculated by numerical integration[9a] of the Lewis–Mayo equation[25] vs. the degree of conversion for poly(acrylamide-*co*-acrylates) prepared in inverse emulsion ($r_A = 0.29$, $r_M = 1.06$, pH 7).[9b] Significant deviations from Bernouillian statistics are observed: the higher the acrylate content, the greater the deviation.

Figure 6 shows a plot of F_A against f_A for samples with f_A in the range $0.15 < f_A < 0.53$ and having degrees of

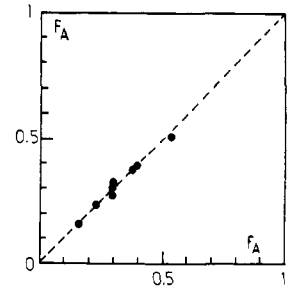

Figure 6. Variation of F_A with f_A for copolymers obtained at low degrees of conversion (<11%).

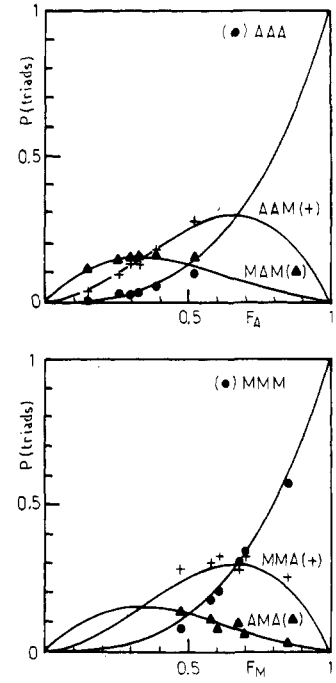

Figure 7. Comparison of experimental triad proportions (symbols) with those calculated for Bernouillian statistics with $P_A = F_A$ (curves) for samples of low degrees of conversion (<11%) (Table III).

conversion lower than 11%. The points to a good approximation lie on the first diagonal corresponding to reactivity ratios $r_A = r_M = 1$.

Figure 7 shows the comparison between the experimental values of the relative triad intensities and the Bernouillian theoretical curves; the agreement is as good

Table IV
Feed Composition (f_A), Copolymer Composition (F_A), Degree of Conversion (Y), and Triad Relative Intensities for the AK Series before and after the Addition of N NaOH

system	Y, %	f_A	F_A	T,[b] °C	N NaOH added, cm³		relative intensity AAA	AAM	MAM	AMA	MMA	MMM
AK-4	4.4	0.226	0.235	19								
			0.334	19	0.2							
			0.319[a]	19	0.2	exptl	0.012	0.109	0.198	0.089	0.378	0.214
						B[c]	0.032	0.139	0.148	0.069	0.296	0.316
AK-6	16.4	0.218	0.249	19								
			0.338	19	0.2							
AK-5	25.6	0.225	0.235	19								
			0.350[a]	80	0.2	exptl	0.027	0.127	0.196	0.086	0.396	0.168
						B[c]	0.043	0.160	0.148	0.080	0.296	0.275
AK-2	71.2	0.227	0.245	19								
			0.347	19	0.2							
			0.336[a]	19	0.2							
AK-3	100	0.226	0.233	19								
			0.347	19	0.2							
			0.346[a]	19	0.2	exptl	0.030	0.112	0.204	0.093	0.386	0.175
						B[c]	0.041	0.157	0.148	0.078	0.296	0.280

[a] Resolution-enhanced spectrum. [b] Temperature of NMR spectrum. [c] Bernouillian.

Table V
Experimental and Calculated Triad Distribution for Low-Conversion Samples

system		relative intensity AAA	AAM	MAM	AMA	MMA	MMM
ZZ-II	exptl	0	0.036	0.114	0.023	0.255	0.572
	B[a]	0.003	0.038	0.108	0.019	0.217	0.614
	M[b]	0.002	0.032	0.119	0.021	0.228	0.604
1C-3Z	exptl	0.018	0.139	0.142	0.051	0.329	0.321
	B[a]	0.027	0.125	0.147	0.063	0.294	0.344
	M[b]	0.025	0.123	0.149	0.063	0.295	0.342
1C-4Z	exptl	0.030	0.126	0.169	0.092	0.283	0.300
	B[a]	0.034	0.143	0.148	0.071	0.296	0.308
	M[b]	0.026	0.132	0.165	0.079	0.304	0.290
C-1	exptl	0.022	0.096	0.144	0.100	0.245	0.393
	B[a]	0.018	0.101	0.143	0.051	0.285	0.402
	M[b]	0.019	0.106	0.144	0.053	0.288	0.387
AB-1	exptl	0.057	0.216	0.147	0.101	0.305	0.174
	B[a]	0.074	0.204	0.141	0.102	0.282	0.195
	M[b]	0.064	0.200	0.154	0.111	0.285	0.183
AB-3	exptl	0.053	0.175	0.165	0.075	0.329	0.203
	B[a]	0.061	0.188	0.145	0.094	0.290	0.224
	M[b]	0.050	0.178	0.159	0.101	0.295	0.215
QY-I	exptl	0.096	0.277	0.141	0.128	0.286	0.072
	B[a]	0.136	0.257	0.121	0.128	0.243	0.115
	M[b]	0.107	0.253	0.150	0.155	0.241	0.094

[a] Bernouillian. [b] Markov.

as that for the samples of high conversion and confirms the random character of monomer placement.

We point out here that the original AK samples were partially neutralized and gave poor spectra from which F_A only could be obtained. It is the value that has been used for AK-4 in Figures 5 and 6. In an attempt to increase the resolution, too much NaOH was inadvertently added, resulting in partial hydrolysis of polyacrylamide and an increase in F_A from 0.23 to 0.35. Triad proportions were nevertheless measured, and the values are compared in Table IV with the predictions of Bernouillian theory by using $P_A = F_A$. The discrepancy in this case is quite marked and outside experimental error (see below). This result agrees with that of other authors[3,20,27] who found that the sequence distribution of acrylamide/acrylate copolymers prepared by alkaline hydrolysis of polyacrylamide is characterized by autoretarded kinetics very different from Bernouillian behavior.

c. Errors and Further Statistical Analysis. Experimental errors were not quoted above in order to avoid excessively complex tables and figures. Here we first consider this vital subject.

The value of F_A is simply obtained from the areas of the A and M signals and is therefore determined with a relatively small error of about 3% because of the clear resolution of the A and M regions. However, the triad intensities are much less reliable because of spectral overlap. Estimates of the errors arising from uncertainties in division of the integrals range from 5% for the better resolved peaks of high intensity, such as MMM in sample A-2 of Figure 2, to 20% for poorly resolved peaks of low intensity, such as AMA in sample A-8 of Figure 2. The agreement with Bernouillian statistics is well within these limits, indicating that the reactivity ratios are both close to unity.

In principle, on the basis of the reactivity ratios described in the Introduction for the acrylamide/acrylate system in other media, one would have expected deviations from Bernouillian statistics significantly greater than the experimental errors. We have analyzed the triad intensities in the low-conversion samples further in terms of first-order Markov statistics in order to compare with the Bernouillian model. The experimental and calculated proportions are given in Table V and the Markov probabilities and reactivity ratios in Table VI. The improvement in agreement of the intensities is marginal, and it is found that $P_{AA} \sim P_{MA}$, $P_{MM} \sim P_{AM}$, and $P_{AM} + P_{MA} \sim 1$. Taking the experimental errors and the scatter of the reactivity ratios between samples into account, we conclude that in this system

$$r_A = 0.89 \pm 0.15 \qquad r_M = 0.92 \pm 0.15$$

Note that the errors in r_A and r_M are not independent since the errors in the triad proportions are not independent. The quoted uncertainties represent the range resulting from reasonable estimate of the uncertainty in the experimental data. There is a positive correlation between r_A and r_M; i.e., higher values of r_A tend to be associated with higher values of r_M.

Discussion

The data presented above clearly indicate that the mechanism of polymerization in microemulsion exhibits characteristics different from those observed in emulsion or in homogeneous solution. The most significant results are the invariance of the average composition of the copolymers with conversion and the conformity of the monomer distribution with Bernouillian statistics.

These conclusions can be related to the mechanism proposed by Candau et al.[10,17] for the polymerization of acrylamide within inverse micelles formed from anionic surfactants (aerosol OT). This procedure is characterized by a very high rate of polymerization (a few minutes) and by a continuous nucleation of the particles uniformly throughout the reaction. The final particle is the result of the fusion of 60–150 micelles and contains on the average *one* single high molecular weight macromolecule, compared with 30 000 chains in inverse latexes.[26] At a given degree of conversion, the medium consists of nucleated polymer particles where the reaction is occurring together with nonnucleated micelles containing monomer. In the present case, the structure of microemulsions before polymerization does not consist of inverse micelles but has a bicontinuous character with an ultralow interfacial tension between the oil and aqueous domains, as shown in another paper.[11] Bicontinuous microemulsions are currently the object of numerous studies[28] and occur when the oil and aqueous contents exist in equivalent amounts, as

Table VI
First-Order Markov Addition Probabilities and Reactivity Ratios for Low-Conversion Samples

system	P_{AM}	P_{MM}	P_{AA}	P_{MA}	$P_{AM} + P_{MA}$	$r_A = r_m$ (B)[a]	r_A (M)[b]	r_M (M)[b]
ZZ-II	0.886	0.842	0.114	0.158	1.03	0.96	0.74	0.98
1C-3Z	0.707	0.697	0.293	0.303	1.01	1.03	1.00	0.95
1C-4Z	0.714	0.656	0.286	0.344	1.06	1.14	0.95	0.80
C-1	0.733	0.729	0.267	0.271	1.00	0.86	0.88	1.10
AB-1	0.607	0.562	0.393	0.438	1.04	1.16	1.04	0.80
AB-3	0.642	0.593	0.358	0.407	1.05	1.01	0.87	0.94
QY-I	0.544	0.438	0.456	0.562	1.11	0.93	0.74	0.88

[a] Bernouillian. [b] Markov.

in this case. However, the bicontinuous structure breaks up as soon as the polymerization starts because of an increase of the interfacial tension. At finite conversion, the system becomes similar to that obtained when the initial microemulsion is of globular type.[17] This explains why in both cases the reaction rates are very high and the final latexes are stable and transparent.

Nevertheless, at this point whether the nucleated particles grow by collisions with nonnucleated micelles or by diffusion of monomers through the organic phase is not resolved. This copolymerization study can be used to distinguish the two processes. For the collision process the monomer proportions at the reaction sites would be maintained throughout the polymerization at their initial values, thus generating a homogeneous microstructure. For the diffusion model, however, the monomer proportions at the reaction sites would depend on the monomer solubilities and diffusion constants in the nonaqueous phase. These would differ between the two monomers, leading to incorporation in the polymer in proportions different from the initial composition. Our observation of a copolymer composition independent of conversion supports the collision mechanism.

In contrast, it appears that the diffusion process is operative in inverse emulsion polymerizations.[14,15] In such systems, the polymerization rate is much lower than in microemulsions (hours as against minutes), and r_A and r_M values are quite different from unity and close to those obtained in aqueous solution.[9] As explained above, the selective reactivity is consistent with the diffusion mechanism. It is possible that the origin of the mechanistic difference lies in the difference in size and number of dispersed particles. Inverse emulsions consist of large monomer droplets ($d \sim 500$ nm) and small micelles ($\sim$ 5–10 nm). It has not yet been firmly established whether the large droplets or the micelles are the polymerization locus in inverse emulsions, but whatever the site, an essential step is the diffusion of monomers from uninitiated reservoir droplets to the active sites.

The second important conclusion concerns the sequence distribution close to a Bernouillian behavior and the values of the reactivity ratios. From Table VI, it appears that the value of r_M is indeed close to that obtained in solution or in emulsion, whereas that of r_A is about 3 times higher. Within the particles the propagation rate constant of the macroradical is high (2×10^4 M^{-1} s^{-1}), but this value is several decades lower than the diffusion constant of the monomers. Other things being equal, it follows that the discrimination between the addition of the two monomers should remain comparable to that in solution and emulsion, and the reactivity ratios should not be modified.

As our results lead to other conclusions, we are forced to attribute that difference to the microenvironment. Exactly which factor leads to the difference in reactivity ratios for the present copolymer system remains unclear. Comparing first of all the microemulsion and solution polymerizations, perhaps the most important difference is that the local concentration of monomers is much higher in microemulsions ($\sim$5 M) than in solution ($\sim$1 M). If the two monomers had significantly different mobilities, the resulting change in viscosity could alter the reactivity ratios to different extents. However, it is difficult to believe that the mobilities of such similar molecules as acrylamide and acrylate could differ sufficiently to explain the observed variation. An alternative explanation may possibly be found in the increased screening of the carboxylate groups by sodium ions in the microemulsions because of the higher ionic strength. This screening would reduce repulsions between neighboring acrylate units and hence increase the probability of AA sequences. The observed increase in r_A in the microemulsions is consistent with this expectation.

Comparing the inverse emulsion and microemulsion data, it is not possible to involve charge-screening arguments because the local concentrations are similar. A possible explanation could arise because of the difference in mechanism. In the inverse emulsions, monomer diffusion from source droplets to the polymerization locus is thought to be an important step. Since the two monomers have different solubilities in the organic phase, their concentrations at the polymerization locus might be different from those in the source droplets. Reactivity ratios obtained by using the droplet concentrations as those of reacting monomers could be apparent rather than true reactivity ratios.

Finally, we note that a further factor meriting consideration is the formation of monomer–monomer complexes which have been shown to have some effect on reactivity ratios[1,2] and which are likely to play an increasingly important role in more concentrated systems.

Acknowledgment. We thank Dr. E. Franta (Institut Charles Sadron), Dr. M. Litt (Case Western Reserve University), and Drs. F. Dawans and J. P. Durand (Institut Français du Pétrole) for stimulating discussions. This work was supported in part by Institut Français du Pétrole and by the PIRSEM (CNRS AIP 2201).

Registry No. (Acrylamide)·(sodium acrylate) (copolymer), 25085-02-3; acrylamide, 79-06-1; sodium acrylate, 7446-81-3.

References and Notes

(1) Plochocka, K. *J. Macromol. Sci., Rev. Macromol. Chem.* **1981**, *C20*, 67.
(2) Kurenkov, V. F.; Myagchenkov, V. A. *Eur. Polym. J.* **1980**, *16*, 1229.
(3) Truong, N. D.; François, J.; Galin, J. C.; Pham, Q. T. *Polymer* **1986**, *27*, 467.
(4) Shawki, S. M.; Hamielec, A. E. *Appl. Polym. Sci.* **1979**, *23*, 3155.
(5) Bourdais, J. *Bull. Soc. Chim. Fr.* **1955**, *22*, 485.
(6) Kabanov, V. A.; Topchiev, D. A.; Karaputadze, T. M. *J. Polym. Sci., Polym. Symp.* **1973**, *42*, 173.
(7) Ponratnam, S.; Kapur, S. L. *Makromol. Chem.* **1977**, *178*, 1029.
(8) Smets, G.; Hesbain, A. M. *J. Polym. Sci.* **1959**, *11*, 217.
(9) (a) Pichot, C. Private communication. (b) Pichot, C.; Graillat, C.; Glukikh, V.; Llauro, M. F. In *Polymer Latex II*; Plastics Rubber Institute: London, 1985; p II/1.
(10) (a) Candau, F.; Leong, Y. S.; Pouyet, G.; Candau, S. *J. Colloid Interface Sci.* **1984**, *101*, 167. (b) Candau, F.; Leong, Y. S.; Kohler, N.; Dawans, F. *Fr.* Patent (to IFP-CNRS) 2 524 895, 1984.
(11) (a) Candau, F.; Zekhnini, Z.; Durand, J. P. *J. Colloid Interface Sci.*, in press. (b) Durand, J. P.; Nicolas, N.; Kohler, N.; Dawans, F.; Candau, F.; French Patent Application (to IFP) 84/08906 and 84/08907, June 1984.
(12) See, for instance, Bellocq, A. M. et al. *Adv. Colloid Interface Sci.* **1984**, *20*, 167.
(13) Vanderhoff, J. W.; Bradley, E. B.; Tarkowski, H. L.; Shaffer, J. B.; Wiley, R. M. "Polymerization and Polycondensation Processes" in *Adv. Chem. Ser.* **1962**, *34*, 32.
(14) Visioli, D. Ph.D Thesis, Lehigh University, Bethlehem, PA, 1984.
(15) Graillat, C.; Pichot, C.; Guyot, A.; El Aasser, M. *J. Polym. Sci., Polym. Chem. Ed.* **1986**, *24*, 427.
(16) Ferrige, A. G.; Lindon, J. C. *J. Magn. Reson.* **1978**, *31*, 337.
(17) Candau, F.; Leong, Y. S.; Fitch, R. M. *J. Polym. Sci., Polym. Chem. Ed.* **1985**, *23*, 193.
(18) Randall, J. C. *Polymer Sequence Determination Carbon-13 NMR Method*; Academic: London, 1977; Chapter 4.
(19) Odian, G. *Principles of Polymerization*; Wiley: New York, 1981; pp 425–433.
(20) Truong, N. D.; Galin, J. C.; François, J.; Pham, Q. T. *Polymer* **1986**, *27*, 459.
(21) Lancaster, J. E.; O'Connor, M. N. *J. Polym. Sci., Polym. Lett. Ed.* **1982**, *20*, 547.

(22) Inoue, Y.; Fukutomi, T.; Chûjô, R. *Polym. J. (Tokyo)* **1983**, *15*, 103.
(23) Zekhnini, Z. Thèse de 3e cycle, Université Louis Pasteur, Strasbourg, 1985.
(24) Moens, J.; Smets, G.; *J. Polym. Sci.* **1957**, *23*, 931.
(25) Mayo, F. R.; Lewis, F. M. *J. Am. Chem. Soc.* **1944**, *66*, 1594.
(26) Reichert, K. H.; Baade, W. *Angew. Makromol. Chem.* **1984**, *123/124*, 361.
(27) Halverson, F.; Lancaster, J. E.; O'Connor, M. N. *Macromolecules* **1985**, *18*, 1139.
(28) Auvray, L.; Cotton, J. P.; Ober, R.; Taupin, C. *J. Phys.* **1984**, *45*, 913.

A ^{13}C NMR Method for Determining the Partitioning of End Groups and Side Branches between the Crystalline and Noncrystalline Regions in Polyethylene

D. L. VanderHart* and E. Pérez

Polymers Division, National Bureau of Standards, Gaithersburg, Maryland 20899.
Received December 30, 1985

ABSTRACT: An ethylene–1-butene linear copolymer (E/B) is shown to give rise to a solid-state ^{13}C spectrum which, when taken with proton–carbon cross polarization (CP), magic-angle spinning, and high-power proton decoupling, contains resolvable resonances from vinyl and methyl end groups as well as ethyl side branches. The signal-to-noise generated after 12–20 h of transient accumulation is sufficient to identify signals of the order of 2 carbons per 10 000 backbone carbons. In contrast to the backbone methylene resonance, which shows shifted, separable signals arising from the crystalline and noncrystalline regions, these weak "defect" resonances show corresponding shifts too small to be definitive. Therefore, the problem of determining the partitioning of defects between the crystalline and noncrystalline regions of polyethylene must be approached indirectly. The method for identifying the morphological origin of defect signals is based on the concept that ^{13}C CP signals are proportional to the local spin polarization levels, which, in turn, are kept quite uniform over distances of nearest neighbors because of proton spin diffusion. Thus, defect signal intensities are argued to be proportional to backbone signal intensities within a given morphological region. By isolating the backbone resonances corresponding to the pure crystalline and noncrystalline components, one thereby isolates the defect resonances. The determination of these pure component line shapes was accomplished by changing the preparation of the proton spin states prior to CP in ways which changed the mixture of crystalline and noncrystalline components in the resulting spectra. Since it is not obvious that the CP efficiency of the backbone carbons and the defect carbons in a given region should be the same, the consistency of the CP intensities with intensities expected based on solution ^{13}C NMR results was probed. In this initial study of the E/B slowly cooled from the melt, the vinyl and methyl end-group carbon resonances were found to have enhancement factors very similar to those of the backbone methylene carbons. The crystalline region, having a mass fraction of 0.76, contained 57% of the methyls and 46% of the vinyls. The fraction of crystalline vinyls in this study is substantially larger than that found in solution-grown crystals in other studies. In contrast, the ethyl-branch carbons were not so well-behaved; i.e., their total intensity was not fully accounted for. Taking account of the missing intensity and the limits of sensitivity, we argue that no more than 20% of the ethyl branches resides in the crystal. On the other hand, there was no direct evidence that any crystalline ethyl branches exist. Studies of this question and others will appear in forthcoming papers.

I. Introduction

^{13}C studies of polyethylene (PE) in solution have yielded a wealth of information about the amount and nature of short-chain branches.[1-4] Long-chain branches are also observed;[1,3-5] moreover, the methyl and α- and β-methylene carbons of saturated chain ends as well as allylic methylene carbons adjacent to terminal vinyl groups are also easily resolved.

Solid-state ^{13}C NMR employing high-power proton decoupling[6,7] and magic-angle spinning[8-11] also yields high-resolution spectra although line widths are typically 10–100 times broader than in solution.[12-15] In contrast to solution spectra, the solid-state spectra may show evidence of heterogeneous environments such as the coexistence of multiple unit cells[16] or the coexistence of crystalline (ordered) and noncrystalline (disordered) regions.[17] The latter consideration dominates the interpretation of the ^{13}C PE spectrum, which, at 50 MHz, typically consists of a sharp crystalline resonance centered at 32.9 ppm[18] and a broader noncrystalline shoulder centered at 31.1 ppm. Since chemical shifts for saturated hydrocarbons in the solid are usually within a few ppm of those found in solution,[19] it is clear from the solution work that several end-group or side-branch resonances (referred to collectively as defect resonances) should be resolvable from the main backbone resonances. In fact, in crystalline *n*-alkanes, the methyl, the α-methylenes, and the β-methylenes are all distinct from the interior methylene resonances.[19] In polyethylene, fewer resonances than in the *n*-alkanes will be distinguishable due to both the much weaker intensity of the defect resonances and the broad, rather intense, noncrystalline resonance. Nevertheless, weak resonances with chemical shifts outside the range of 26–38 ppm are expected to be visible. This includes all methyls, α-methylenes (marginal), methine branch carbons (marginal), and vinyl carbons (terminal and interior). Therefore, the observation of these resonances is possible, in principle. The only questions are those of sensitivity and cross-polarization (CP) efficiency.

The advantage of the solid-state ^{13}C measurements compared with liquid-state studies, therefore, is that the solid-state morphology is present. In this paper we do not seek to argue for the superiority of the solid-state approach over liquid-state methods in determining defect concentration. Rather, we seek to probe the *location* of the defect resonances, i.e., how the side groups and end groups are

0024-9297/86/2219-1902$01.50/0